Texture-Based Weed Classification Using Gabor Wavelets and Neural Network for Real-time Selective Herbicide Applications

L. Tang, L.F. Tian, B.L. Steward and J.F. Reid

Department of Agricultural Engineering
University of Illinois at Urbana-Champaign
Urbana, IL 61801

ABSTRACT

A novel texture-based weed classification method was developed. The method comprised a low-level Gabor wavelets-based feature extraction algorithm and a high-level neural network-based pattern recognition algorithm. The design strategy simulated the function of the human visual system, which uses low-level receptors for early stage vision processing and high-level cognition for pattern recognition and image understanding. This model was specifically developed to classify images into broadleaf and grass categories for real-time selective herbicide application. The results showed that the method is capable of performing texture-based broadleaf and grass classification effectively and with 100 percent classification accuracy over 40 sample images with 20 samples from each class. Based on the elapsed time to do weed classification, the method meets real-time constraints.

1. INTRODUCTION

In post-emergence applications, broadleaf and grass species are typically controlled differently with selective herbicides or with different tank mixes and application rate of non-selective herbicides (Novartis, 1998). Thus with the growing use of selective application technologies, if locally sensed field areas could be classified as being infested with broadleafs or grasses, then the appropriate strategy for broadleaf and grass control could be selectively applied. This is one step beyond selective herbicide application based on presence or absence of weeds in a local area, thus, leading to more effective post-emergence herbicide application.

Research on weed or plant identification and weed classification basically falls into two categories; that using shape-based classification and that using texture-based classification. Shape feature-based weed species classification has been conducted by numerous researchers (Guyer et al., 1986, 1993; Franz et al., 1990; Woebbecke et al., 1995b; Zhang and Chaisattapagon, 1995; Yonekawa et al., 1996). This type of method has limited application to whole canopies as it demands analysis on the individual seedling or leaf level. Texture features of weed species have been applied in distinguishing weed species by Meyer et al. (1998). In this research, four classical textural features derived from the co-occurrence were used for discriminant analyses. Grass and broadleaf classification had accuracy of 93% and 85%, respectively. Individual species classification accuracy ranged from 30% to 77%. An overall system response time of 20 to 30 seconds on UNIX computer system with KBVision was reported.

In more general texture research, Haralick et al. (1973) used co-occurrence matrices to classify sandstone categories in photomicrograph images and wood, lake, road, etc., in aerial images. Davis et al. (1979) indicated that using co-occurrence matrices for complex texture analysis is computationally intensive. Statistical methods, like using co-occurrence spatial

dependence statistics, have been in the past proven superior to frequency domain techniques (Weszka et al., 1976). In fact, this is due to the lack of locality in early frequency analysis methods. Reed and Hans Du Buf (1993) concluded that joint spatial/spatial-frequency techniques are inherently local in nature, and have characteristics superior to those of the statistical methods.

Joint spatial/spatial-frequency methods are able to indicate the frequency content in localized regions in the spatial domain. These methods can overcome the drawbacks of traditional Fourier-based techniques, which can only provide global spatial frequency information. When local features are extracted instead of the global ones, the detection of continuity of a feature as well as the edges between different regions is consequently enabled. Experiments on the human visual system have shown that both retinal and cortical cells can be characterized as having limited extent of receptive field, and as such can be described as local feature extractors. Thus, cortical simple cells have been described as bar or edge detectors (Porat and Zeevi, 1989). Daugman (1985) indicated that Gabor wavelets resemble the receptive field profile of the simple cortex cells. Bovik et al. (1990) further emphasized that 2-D Gabor filters have been shown to be particularly useful for analyzing texture images containing highly specific frequency or orientation characteristics.

Based on the research cited above, the potential of using joint spatial/spatial frequency texture features to do weed classification exists. Little research effort with this approach has been seen so far. An algorithm using this method could effectively classify weeds with varying canopy size and with high computational efficiency. Such an algorithm is needed for real-time selective herbicide applications and thus should be explored. These considerations provided motivation for this research study.

2. OBJECTIVES

The objectives of this research were to explore the feasibility of using Gabor wavelet-constructed spatial filters to extract texture-based features from field images consisting of broadleafs and grasses, and to use these extracted feature vectors to train and test a neural network classifier. To evaluate the robustness of the method, images with natural weed cluster patterns taken from a camera under natural outdoor lighting conditions were used. The objectives were accomplished by the following tests:

- Collection of an image database representing broadleaf and grass images under natural field and lighting conditions.
- Creation of a feature extractor based on a Gabor wavelet filter-bank.
- Development of a neural network classifier to do pattern recognition based on these features.
- Evaluation of algorithm classification accuracy and computational efficiency.

3. MATERIALS

Three broadleaf species -- common cocklebur, velvetleaf and ivyleaf morningglory, and two grass species -- foxtail and crabgrass were planted at the University of Illinois Agricultural Engineering Research Farm on May 28, 1999. Each species was planted in a small plot, which measured 1.2 m by 3.6 m (4 ft by 12 ft). Images were taken on June 30, 1999, which was about four weeks after planting. This growth stage was that which would be encountered at the common post-emergence herbicide application time. A ViCAM USB video conferencing digital camera (Vista Imaging Inc., San Carlos, CA) and a Compaq Presario laptop 1655 computer with a 266 MHz Pentium II processor were used to grab a series of images. ViCAM camera was mounted on

tripod at height of 1.4 m (55 in). The camera had a pixel resolution of 640 by 480. The camera was equipped with a standard ViCAM lens, which had a 6.5mm focal length and a F2.0 relative aperture. The lens had a 44 degree horizontal viewing angle and a 32 degree vertical viewing angle. Thus the field of view measured 1.1 m by 0.8 m (44 in. by 32 in.), which resulted in a resolution of approximately 1.7 mm by 1.7 mm per pixel (0.07 in by 0.07 in per pixel). ViCAM camera was manually white balanced with 86 percent red, 31 percent blue and 50 percent color level settings. The auto white balance was turned off. The auto gain control was set at the peak mode, and the image quality control was set at the high quality setting with 24-bit RGB color. The lighting intensity and color temperature levels were recorded by using chroma meter (Model No. xy-1, Minolta Co., ltd., Ramsey, New Jersey, U.S.A.). During the whole image collection period, the intensity and color temperature levels varied from 14000 lux to 90000 lux and from 5800 K to 7150 K respectively. The shutter speed varied from 1/240 s to 1/3500 s corresponding to the minimum and maximum intensity level. In total a set of ten velvetleaf, four ivyleaf morningglory, six common cocklebur, ten foxtail and ten crabgrass images were generated by cropping 300x250 portions from images of size 640x480. The ViCAM camera used a conventional CCD sensor, but its low cost lens created blurring at the four image corners. Thus only portions from the center of images were cropped as sample images.

The feature extraction algorithm was written in Microsoft Visual C++ 6.0 (MicroSoft Corp., Redmond, WA). Neural network classification was done using Matlab version 4.0 (The MathWorks, Inc., Natick, MA).

4. METHODS

A novel wavelet/neural network system was developed to accomplish the texture-based broadleaf and grass classification task. There were two layers in this scheme. A Gabor wavelet-based algorithm that extracted spatial/spatial-frequency features of the weed images. A feedforward neural network that processed the extracted feature vectors to perform the weed classification task.

4.1. IMAGE PRE-PROCESSING

Compared with general texture analysis applications, texture-based weed classification has particular characteristics. Weed texture patterns can vary greatly from image to image depending on weed species, density and location in the images. Background features should be eliminated to extract spatial frequency features from the weeds. Meyer et al. (1998) indicated that weeds in field images must be carefully segmented, otherwise the textural analysis will yield unreliable results from analyzing soil and plant features as weeds. Thus, adequate image segmentation quality is necessary. Segmented images were used to constrain sampling to ensure sampling points, which were the central locations of later on convolution filtering, from known vegetation regions. Woebbecke et al. (1995a) examined several color indices for weed image segmentation and found excess green (ExG) and modified hue yielded the best near-binary images of weeds. Meyer et al. (1998) applied ExG to separate plant and soil region for weed species identification research as well. The color index used for segmentation in this research was called Modified Excess Green (MExG). MExG was defined as:

$$ExG = 2 * G - R - B \tag{1}$$

with constraints: if (G<R or G<B or G<120), then ExG=0.

where R, G, B were the unnormalized red, green and blue intensities of a pixel.

The modification of the excess green color index was motivated by the occurrence of image artifacts generated by the ViCAM camera used in this research. The color saturation tended to rise at the edges of the plants in images. It also brought red, blue channel signal to a very low value in some background area where the intensity level was changing rapidly. To overcome these color artifacts, the two constraints were added to ExG equation.

The segmentation threshold was determined by examining the MExG histogram 'valleys' and also adjusted by visually observing segmentation results using user interactive display function from software Image-Pro Plus 3.0 (Median Cybernetics, Silver Spring, MD). The threshold was chosen as 25 for all images. Example weed images and their MExG and segmented images are shown in Figure 1.

4.2. FEATURE EXTRACTION USING GABOR WAVELETS

The development of this Gabor wavelet feature extractor was motivated by the fact that Gabor wavelets have been shown to resemble the receptive field profile of simple visual cortex cells, which can perform joint spatial/spatial frequency analysis (Porat and Zeevi, 1989; Bovik et al., 1990, 1992; Reed et al., 1993; Mallat, 1996; Naghdy et al., 1996). The general reasoning of the choice of Gabor wavelets as feature extractor follows the development of Naghdy (1996).

In order to briefly describe Gabor wavelets and provide a rationale for this research, the Short Time Fourier Transform (STFT) and Gabor Transform need to be explained first. The Fourier transform is a fundamental tool of classical signal analysis. The Fourier transform is defined as follows:

$$F(w) = \int_{-\infty}^{+\infty} f(t)\exp(-jwt)dt \tag{2}$$

where $F(w)$ is the Fourier transform of the time basis signal $f(t)$, and

$$\exp(jwt) = \cos(wt) + j\sin(wt) \tag{3}$$

The Fourier transform can only provide signal information in the frequency domain without any localized references to the time domain. Human vision model research has suggested the existence of an internal spatial/frequency representation that is capable of preserving both local and global information (Beck et al., 1987). With the Fourier transform, it is not possible to do joint spatial/spatial-frequency analysis. In contrast, STFT can achieve this function and it is defined as:

$$STFT(t,w) = \int s(t)g(t-t)\exp(-jwt)dt \tag{4}$$

From this definition, the STFT can be interpreted as the Fourier transform of a signal that is windowed by the function $g(t-t)$. The STFT with a Gaussian window is called a Gabor Transform. The Gabor Transform can be regarded as a signal being convolved with a filter-bank, whose impulse response in the time domain is Gaussian modulated by sine and cosine wave. As the frequency (w) of the sine and cosine function changes, a set of filters with the same window size is constructed. The problem with the STFT or Gabor Transform is that the size of the window in the time domain is fixed, and thus results in a fixed resolution in both spatial and frequency domains. Therefore, the STFT and Gabor Transform are suitable for analysis of stationary signals, which is not the case of most of natural textures. This problem can be overcome by the wavelet transform.

A wavelet is defined as:

$$h_{b,a}(t) = \frac{1}{\sqrt{a}} h^*(\frac{t-b}{a}) \tag{5}$$

and the continuous wavelet transform is defined as:

$$CWT(b,a) = \frac{1}{\sqrt{a}} \int_{-\infty}^{+\infty} h^*(\frac{t-b}{a}) s(t) dt \tag{6}$$

where $s(t)$ is the signal, a and b are the dilation and translation factors respectively and $h(t)$ is called the mother wavelet. The wavelet transform is to decompose the signal $s(t)$ into the set of wavelet functions. The wavelet transform obtains a flexible resolution in both time/spatial and frequency domain through factors a and b.

The two-dimensional Gabor elementary function is defined as:

$$g(x,y) = \frac{1}{2p} \exp[\frac{x^2+y^2}{s^2}] \cdot \exp[j2pw_0(x\cos q + y\sin q)] \tag{7}$$

where s is the variance of Gaussian distribution in both the x and y directions, w_0 is the frequency of the sinusoid, and q is the orientation of the sinusoid. The Gabor element function actually is a two-dimensional Gaussian envelope modulated by a sinusoid with the frequency w_0 and orientation q.

In this research, the Gabor wavelet function used for weed feature extraction was same as Naghdy (1996) used and was defined as:

$$h(x,y) = \exp[-a^{2j} \frac{x^2+y^2}{2}] \cdot \exp[jpa^j(x\cos q + y\sin q)] \tag{8}$$

where $a = \frac{1}{\sqrt{2}}$, $j = 0,1,2\ldots$ and $q \in [0,2p]$ The different choices of frequency j and orientation q constructed a set of filters.

As the frequency of the sinusoid changes, the window size will be changed. Figure 2 shows real and imaginary parts of eight two-dimensional wavelets filters. When j is changed from 0 to 3, the sinusoid frequency is reduced whereas the Gaussian window size increases. In comparison, for the Gabor transform, Gaussian window size will remain same.

The elementary Gabor wavelet functions were used to construct spatial domain filters. Each filter was made of a pair of filters which were the real and imaginary part of the complex sinusoid. These pair were convoled with the green channel signal of texture image separately. The reason of choosing the green channel to do convolution was that the green channel was found to have the best texture quality, which means the best contrast level between plants and soil, among red, blue and MExG channels. This scenario is absolutely sensor dependent and may not be the case for other sensors. For one frequency level, the filtering output was the modulation of the average of the convolution output from real and imaginary filter masks on all convolved pixels in the green channel image, which was computed as:

$$Output = \sqrt{R_{ave}^2 + I_{ave}^2} \tag{9}$$

where R_{ave} is the result of the convolution of the sample image region with the real filter mask and I_{ave} is the result of the convolution of the sample image region with the imaginary filter mask.

This equation means every complex filter pair for one frequency level was employed to capture one feature of a texture. For each weed image, a multidimensional feature vector was constructed based upon the filters used.

4.3. FILTER FREQUENCY AND CONVOLUTION MASK SIZE ANALYSIS

In order to distinguish broadleaf and grass effectively and efficiently, a specific filter-bank with proper frequency levels and suitable filter dimension (i.e. a convolution mask size) was determined through experiments. A set of sample images of all five weed species were selected to do the experiment. Ten frequency levels from zero to nine and three mask sizes of 9 by 9 pixels, 13 by 13 pixels and 17 by 17 pixels were used to measure the effect of frequency level and mask size on the suitability various features and seperability of the two classes. Feature vectors were clearly affected by the frequency level and mask size (Figures 3, 4, and 5). To reduce the computational load, the filter-banks should be made as small as possible as long as adequate distinguishable information can be provided for a high-level classifier. By analyzing the curves, a filter-bank with four frequency levels from three to six was determined to be the most suitable for the classification task. Mask size affects the amount of computation needed to extract the features as well as classification accuracy. Generally, a larger mask size will be able to pick up more details in the texture image, but for real-time application consideration, the mask size needs to be minimized. In this research, a mask size of 17 pixels by 17 pixels was selected. The number of convolution points also directly affects the computational load. During the experiments, features were generated based on 100, 150 and 200 random convolution points, and some substantial differences were observed on in the feature vectors from some weed images when the number of points was 100. When 150 and 200 random points used, minor differences were observed. Thus 150 was chosen as the number of total random convolution points in the green channel image. Random points were selected with the constraint that the pixel value in MExG channel at these points must be greater than the threshold 25. These random convolution points were the center points where the images convolved with Gabor wavelets filter masks. Figure 6 illustrates the feature vectors extracted by using above parameters. The weed classes appeared to be separable based on these feature vectors. The filter-bank used in this research is depicted in Figure 7. As a summary of feature extraction algorithm, a stepwise block diagram can be referenced in Figure 8.

4.4. NEURAL NET WORK CLASSIFICATION

A three-layer feedforward backpropagation Artificial Neural Network (ANN) was built by using the Matlab® neural network toolbox. Multilayer networks trained by the backpropagation algorithm are capable of learning nonlinear decision surfaces and thus make efficient and compact classifiers. The ANN was trained until the sum square error of 0.01 being reached as the final learning convergence criterion. The input feature vector matrix had a size 4 by 20 elements, so the network had 4 input layer nodes. The hidden layer consisted of eight nodes. The output layer had two nodes, which corresponded to the two broadleaf and grass classes. The logarithmic sigmoid function was chosen as the threshold unit for all three layers and the learning rate was set to one.

5. RESULTS AND DISCUSSION

In total, 40 weed images including individual classes of common cocklebur, velvetleaf, ivyleaf morningglory, crabgrass and giant foxtail were classified. All images were processed with the Gabor wavelets feature extractor, and the feature vectors were saved to a file before neural network training. Twenty images with ten images from each group were used to train the neural network classifier; the remaining 20 images were used as validation images and were classified.

The ANN training process converged quickly within 500 epochs. Both the training data and test data set were classified with 100 percent accuracy. Table 1 lists the classification output for the test image set.

This research was intended to explore the feasibility of the methodology described in this paper. In the current system, there are several limitations, and correspondingly, several potential improvements can be listed. First, the feature extraction algorithm only applies unidirectional wavelet filters. This implies that the algorithm requires a difference in the width of broadleaf and grass leaves along a single direction. Although it is typically the case that broadleaf leaves are wider than grass leaves, it is not always true. The main difference between broadleaf leaves and grass leaves is that broadleaf leaves have rounded or slightly elliptic shapes whereas grass leaves have elongated shapes. Asymmetric filter mask or multiple orientation filter masks with different mask size and frequency combinations could possibly pick up local spatial frequency changes, which are more pertinent to the natural difference between these two weed classes.

Second, each weed image in this initial research has only one weed species. Though several same class species in one image may not affect broadleaf and grass classification task, the case of more than one classes presenting in one image has not been investigated. In case of the multiple species images, which can happen frequently under field conditions, a method of texture-based segmentation, instead of just a classification, needs to be developed. This will be a next step of this weed classification research. One possible adaptation of this classification algorithm is to find the near minimum broadleaf or grass cluster size, from which the current classification algorithm can still extract separable features from this reduced weed area. Then this area could be used as a scanning unit, and the image could thus be segmented into broadleaf and grass areas at the resolution level of this basic unit based on the current classification algorithm.

Third, a fixed image resolution level was used in this research. For practical agricultural applications, it is important to consider ways to lower the cost of sensing equipment. Although the camera had a field of view of about one and a half crop row spacing, larger fields of view would lower the number of sensors required for a particular implementation. Therefore, classification evaluation at near sensor limitation level can reveal that how large area one sensor can cover without affecting this classification performance over an acceptable range.

The algorithm using this feature extraction scheme is computationally efficient. For example, consider the case of an image of consisting of 300 by 250 pixels. With four frequency levels, there will be eight filter masks from both real and imaginary parts. With 150 random convolution points and mask size of 17 by 17 pixels, the number of calculations will be 17x17x8x150, which is '2-D mask size' times 'mask number' times 'convolution points', and thus results in 346800 multiplications. Comparing this computation load with a simple one run low-pass or high-pass filtering with a three by three pixel filter mask, the number of computations will be 298x248x3x3, ('edge trimmed image size' times 'filter size'). This filter operation thus results in 665136 multiplications, which is about double the computation required for the feature extraction scheme. The time expense on feature extraction for one weed image including all image pre-processing steps was measured. The average value was around 550 milliseconds measured on Pentium II 233 MHz computer. The major part of image pre-processing was to create a MExG image for segmentation. Time can be saved from this processing by using a look-up table, which uses computer memory to trade speed (Tian and Slaughter, 1998; Steward and Tian, 1998).

A low-cost video conferencing color camera was used to collect weed images. The automatic functions provided by camera driver were useful to cope with outdoor lighting conditions. The auto gain control was especially effective in dealing with dramatic lighting intensity changes that often

occur during the day. Although this camera has limitation in data transfer rate due to its use of the universal serial bus (USB), which has maximum baud rate 12 million bits per second, the camera can still acquire 8 frames per second in medium quality mode (single field mode) when it is connected to a 230 MHz computer. The color artifacts created by the simple lens will reduce the useable region of image, but it can still cover one or two inter crop-row region with acceptable resolution for agriculturally-based applications. The image quality of the set of images used in this research was stable over a daytime long period of collection.

6. CONCLUSIONS

In this paper, a two-layer wavelet feature extraction and neural network pattern recognition system, which simulated processes of the human visual system was established to classify weed into broadleaf and grass classes for real-time selective herbicide application. Gabor wavelets were applied to obtain the joint spatial/spatial-frequency characteristics of the weed texture images. This Gabor wavelets feature extractor simulated the function of visual cortex cells. A feedforward backpropagation neural network simulated high-level brain learning and recognition process. This system achieved a 100 percent classification accuracy. The feature extraction algorithm was computationally efficient and can meet real-time application requirements. Therefore, this system can be concluded as a promising technique for broadleaf and grass classification**.**

7. ACKNOWLEDGMENTS

The authors would like to acknowledge and thank the Illinois Council on Food and Agricultural Research (Project No. 99I-112-3AE) for the support of this research. A special thanks goes to our colleague, Haibo Yao, for his great help on weeds planting and image collection work.

The use of trade names is only meant to provide specific information to the reader, and does not constitute endorsement by the University of Illinois.

8. REFERENCES

Beck, J. A. Sutter and R. Ivry. 1987. Spatial frequency channels and perceptual grouping in texture segregation. *Computer Vision, Graphics, and Image Processing* 37: 299-325.

Bovik, A.C., M. Clark, and W. Geisler. 1990. Multichannel texture analysis using localized spatial filters. *IEEE Transaction on Pattern Analysis and Machine Intelligence* 12: 55-73

Bovik, A.C., N. Gopal, T. Emmoth and A. Restrepo. 1992. Localized measurement of emergent image frequencies by Gabor wavelets. *IEEE Transactions on Information Theory* 38(2): 691-712.

Daugman, J.G. 1985. Uncertainty relation for resolution in space, spatial frequency, and orientation optimized by two-dimensional visual cortical filters. *Journal of the Optical Society of America A.*, 2(7): 1160-1169.

Davis, L.S., S.A. Johns, and J.K.Aggarwal. 1979. Texture analysis using generalized co-occurrence matrices. *IEEE Transaction on Pattern Analysis and Machine Intelligence* 1:252-259.

Franz, E., M.R. Gebhardt, and K.B. Unklesbay. 1991. The use of local spectral properties of leaves as an aid for identification weed seedlings in digital images. *Transactions of the ASAE* 32(2): 682-687.

Guyer, D.E., G.E. Miles, L.D. Gaulttney, and M.M. Schreiber. 1993. Application of machine vision to shape analysis in leaf and plant identification. *Transactions of the ASAE* 36(1): 163-171.

Guyer, D.E., G.E. Miles, M.M. Shreiber, O.R. Mitchell, and V.C. Vanderbilt. 1986. Machine vision and image processing for plant identification. *Transactions of the ASAE* 29(6): 1500-1507.

Haralick, R.M., K. Shanmugam, and I. Dinstein. 1973. Textural features for images classification. *IEE Transactions on systems, man, and cybernetics.* 3:610-621.

Mallat, S. 1996. Wavelets for a vision. *Proceedings of the IEEE*, 84(4): 604-614.

Meyer, G.E., T. Mehta, M.F. Kocher, D.A. Mortensen, A. Samal. 1998. Textural imaging and discriminant analysis for distinguishing weeds for spot spraying. *Transactions of the ASAE* 41(4): 1189-1197.

Naghdy, G., J. wang, and P. Ogunbona. 1996. Texture analysis using Gabor wavelets. *IS&T/SPIE Symp. Electronic Imaging. Proc. SPIE* 2657: 74-85

Novartis. 1998. *Sample labels and reference guide*. Novartis, Greensboro, North Carolina.

Porat, M. and Y. Y. Zeevi. 1989. Localized texture processing in vision: analysis and synthesis in the Gaborian space. *IEEE Transactions on Biomedical Engineering*, 36(1): 115-129.

Reed, T.R., J.M. Hans Du Buf. 1993. A review of recent texture segmentation and feature extraction techniques. *Computer Vision Graphics and Image Processing: Image Understanding*. 57(3): 359-372

Steward, B.L. and L.F. Tian. 1998. Real-time weed detection in outdoor field conditions. *In proc. SPIE 3543, Precision Agriculture and Biological Quality*, eds. G.E. Meyer and J.A. DeShazer, 266-278. Bellingham, Wash.:SPIE.

Tian, L.F. and D.C. Slaughter. 1998. Environmentally adaptive segmentation algorithm for outdoor image segmentation. *Computers and Electronics in Agriculture* 21(3): 153-168.

Wechsler, H. 1982.Texture analysis--A survey. Signal Proc., 2: 271-282

Weszka, J.S., C.R. Dyer, and A. Rosenfeld. 1976. A comparative study of texture measures for terrain classification. *IEE Transactions on systems, man, and cybernetics* 6: 269-285

Woebbecke, D.M., G.E. Meyer, K. Von Bargen, and D.A. Mortensen. 1995a. Color indices for weed identification under various soil, residue, and lighting conditions. *Transactions of the ASAE* 38(1): 259-269

Woebbecke, D.M., G.E. Meyer, K. Von Bargen, and D.A. Mortensen. 1995b. Shape features for identifying young weeds using image analysis. *Transactions of the ASAE* 38(1): 271-281.

Yonekawa, S., N. Sakai, and O. Kitani, 1996. Identification of idealized leaf types using simple dimensionless shape factors by image analysis. *Transactions of the ASAE* 39(4): 1525-1533.

Zhang, N. and C. Chaisattapagon. 1995. Effective criteria for weed identification in wheat fields using machine vision. *Transactions of the ASAE* 38(3): 965-974.

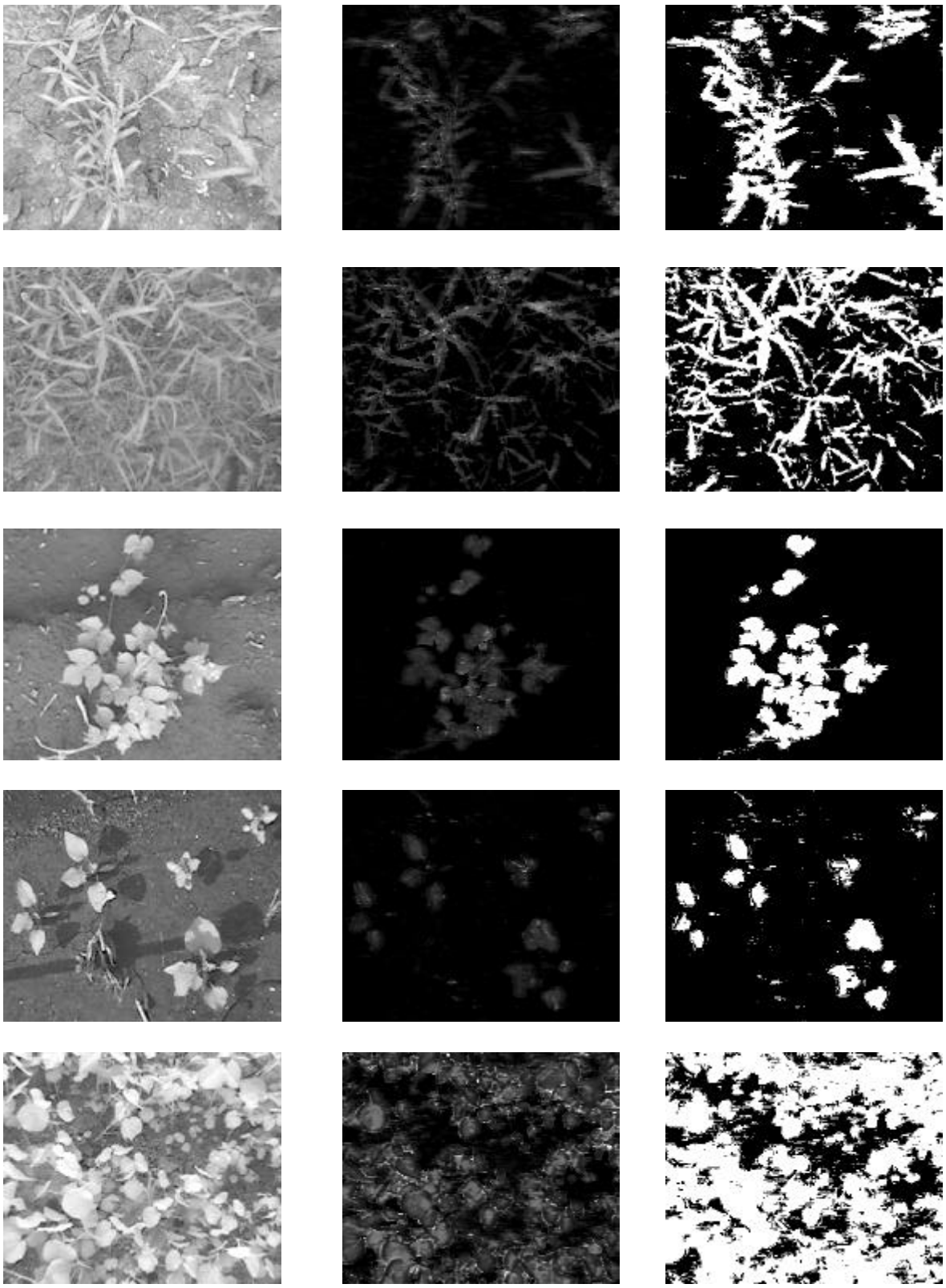

Figure 1. Typical images and image segmentation results. From the top to bottom row, the images represent crabgrass, foxtail, ivyleaf morningglory, common cocklebur and velvetleaf consequently. From the left to right columns, images represent green channel images, modified excess green images and segmented images with a threshold 25.

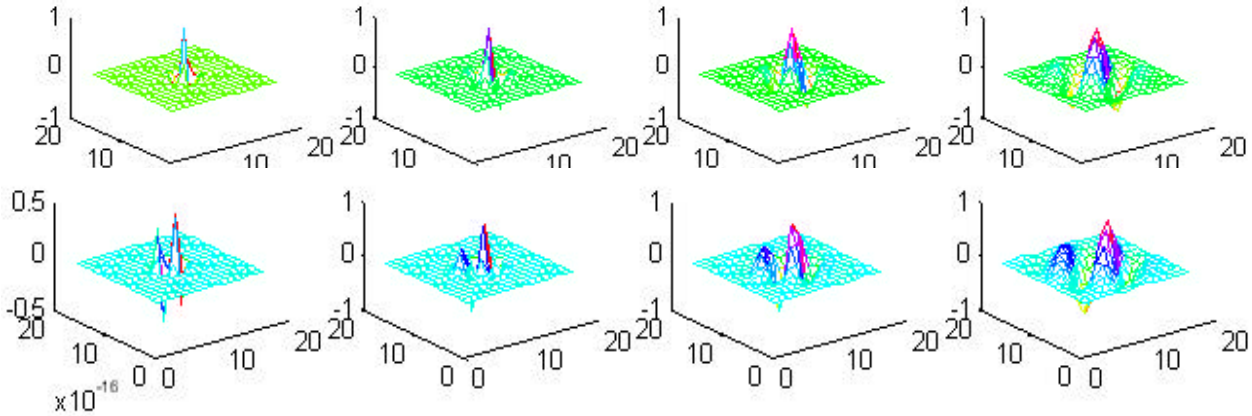

Figure 2. Perspective views of real (top row) and imaginary (bottom) components of 2-D Gabor filters at orientation 90° with frequency level j changing from 0 to 3 (left most to right most at each row)

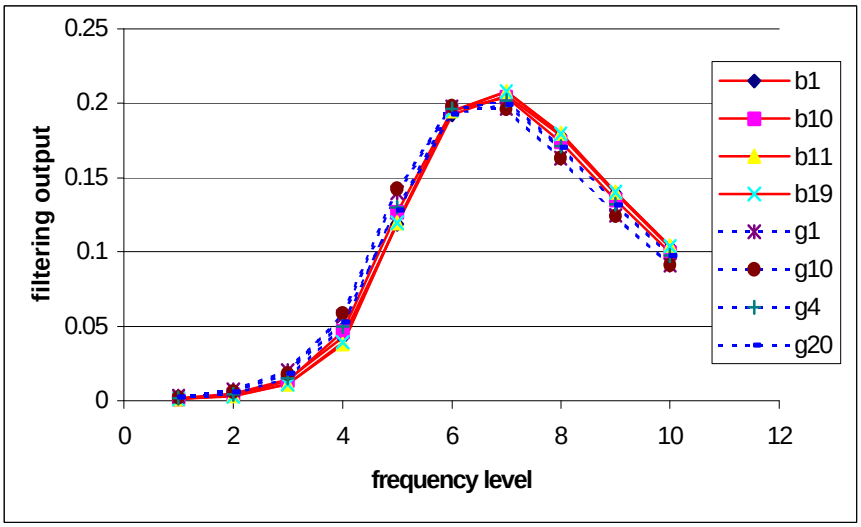

Figure 3. Feature vectors with 10 frequency level and mask size 9x9. 'b' -- broadleaf, 'g' -- grass

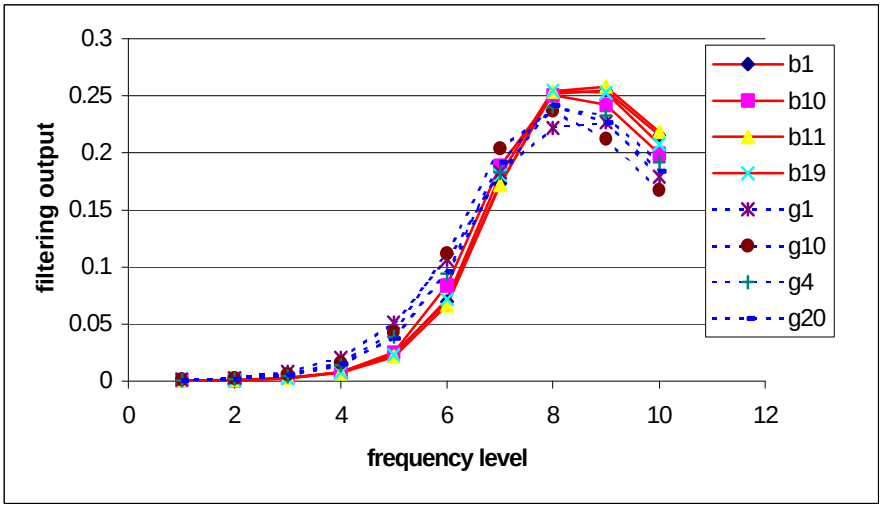

Figure 4. Feature vectors with 10 frequency level and mask size 13x13. 'b' -- broadleaf, 'g' -- grass

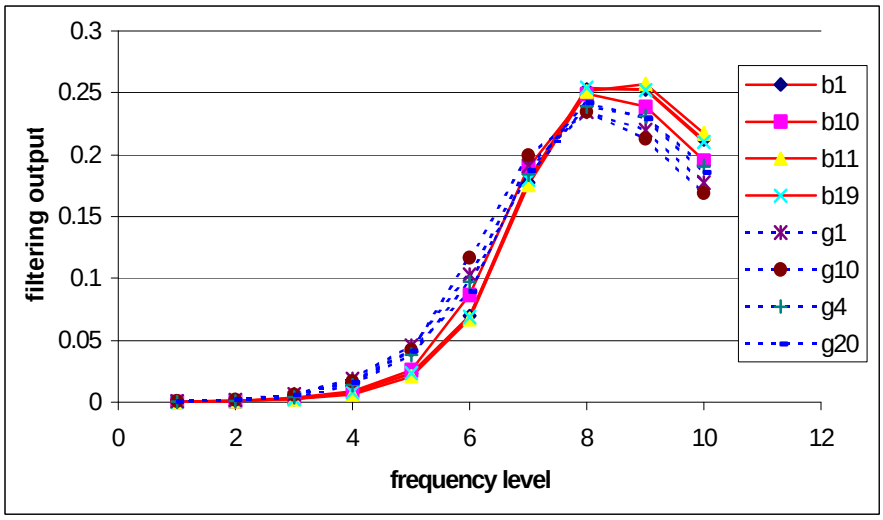

Figure 5. Feature vectors with 10 frequency level and mask size 17x17. 'b' -- broadleaf, 'g' -- grass

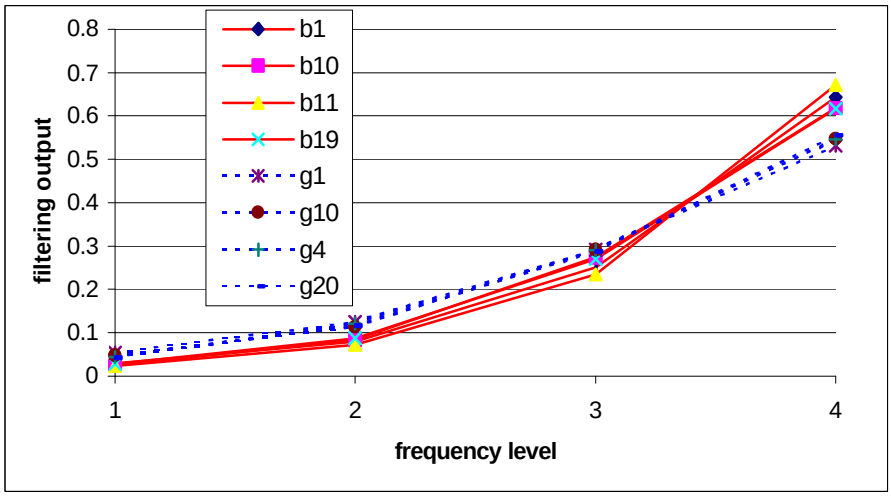

Figure 6. Feature vectors with frequency level 3 - 6 and mask size 17x17. 'b' -- broadleaf, 'g' -- grass

Figure 7. Filter-bank used in this research. From left to right, frequency level j changes from 3 to 6. Top and bottom rows are real and imaginary components, respectively. Filter mask size is 17x17.

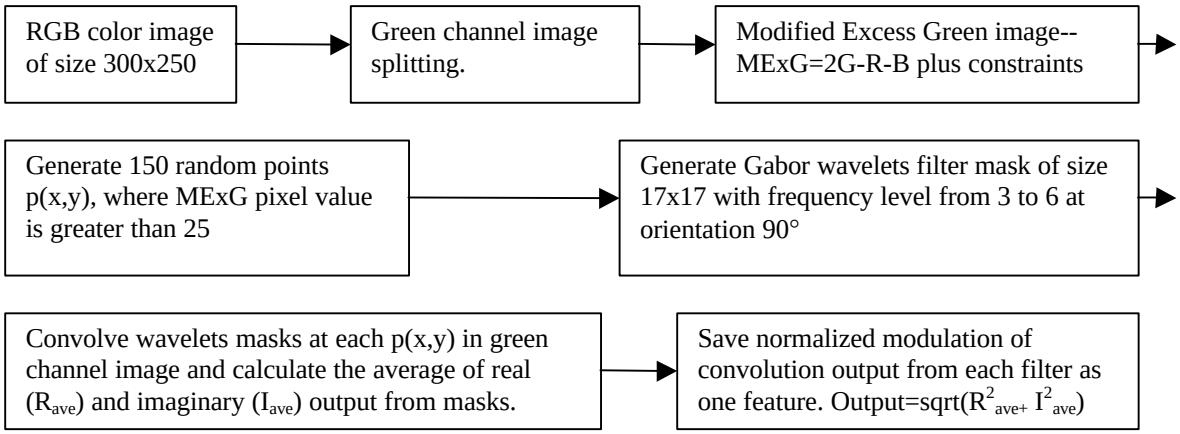

Figure 8. Block diagram of image pre-processing and feature extraction algorithm

Table 1. Classification results from neural network. 'B' --broadleaf, 'G' -- grass

	B1	B2	B3	B4	B5	B6	B7	B8	B9	B10
broadleaf	0.9939	0.9939	0.9939	0.9939	0.9939	0.9939	0.9939	0.9954	0.9954	0.9892
grass	0.0048	0.0154	0.0039	0.0074	0.0049	0.0034	0.0037	0.0037	0.004	0.0079

	G1	G2	G3	G4	G5	G6	G7	G8	G9	G10
broadleaf	0.0102	0.0082	0.0075	0.0078	0.0065	0.0375	0.0312	0.0064	0.0061	0.043
grass	0.9921	0.9929	0.9957	0.995	0.9951	0.9616	0.9597	0.9967	0.9962	0.9583